EurJIC
European Journal of Inorganic Chemistry

Research Article
doi.org/10.1002/ejic.202400690

Chemistry Europe
European Chemical Societies Publishing

www.eurjic.org

A Hobson's Choice Co-Ligand in Imparting Spin Crossover in Fe(II) Complexes Based on 1,3,4-Oxadiazole Ligands

Sriram Sundaresan,*[a] Julian Eppelsheimer,[a] Luca M. Carrella,[a] and Eva Rentschler*[a]

In this manuscript we report the synthesis of three methanol solvatomorphs of Fe(II) complexes with the 2-(2-phenyl)-5-[N,N-bis(2-pyridylmethyl)aminomethyl]-1,3,4-oxadiazole (L^{Ph-ODA}) ligand and three different NCE co-ligands where E=S, Se and BH_3 (**C1**–**C3**). The complexes obtained were characterized by single crystal X-ray crystallography and SQUID magnetometry between 2 and 300 K. Complexes **C1** and **C2** remain in the high spin state over the entire measured temperature window, whereas complex **C3** exhibits a solvent dependent spin transition with a $T_{1/2}$ of 166 K. Upon heating the sample to 400 K and removing methanol, the complex exhibited a two-step spin transition with the first step having a $T_{1/2}$ of 215 K and a second step having a $T_{1/2}$ of 137 K.

Introduction

Molecules exhibiting spin crossover (SCO) properties are a class of switchable molecules which emerges to be promising candidates for several potential application including displays and data storage.[1–4] Over the past decade, the use of spin transition materials has been extended to new areas of applications, including sensors, molecular actuators and more recently solving complex mathematical problems of generating true random numbers instead of software generated pseudo random numbers.[5,6] The interplay between the SCO and solvatomorphism in the solid-state facilitates the potential use of these SCO materials as solvent sensors.[7–9] These materials can act as solvent sensors whereby incorporation of different solvent into the lattice of an SCO complex leads to a distinct change in the colour as well as the magnetic properties of the complex. This property can be harnessed to detect and differentiate between various solvents based on measurable changes in the magnetic, optical as well as electronic properties.[10,11] Understanding and controlling these effects can lead to the development of sophisticated materials for sensor technologies and other applications requiring precise environmental responsiveness.[3,12]

Fe(II) complexes based on 1,3,4-Oxadiazole ligands are seldom reported in the literature for SCO. In 2016 we reported the first oxadiazole based dinuclear Fe(II) complex with SCO properties and also investigated the crystal packing effects by the choice of three different anions.[13] Further fine tunings of the ligand design to move the spin transition temperature close to room temperature were not successful as the complexes, irrespective of the counter ions chosen, were locked in HS state.[14] The attempts made by Klingele and co-workers as well as Herchel and co-workers with bis bidentate ligands along with the NCS co-ligands always yielded mononuclear complexes of Fe(II) locked in HS state.[15,16] In 2023, we reported the first Fe(II) mononuclear complex with a tetradentate 1,3,4-oxadiazole ligand with $NCBH_3$ co-ligands, which shows spin transition in both solid state and solution.[17] A more detailed study of the effect of the co-ligands as well as ligand substituents was reported earlier this year.[18] The DFT calculations as part of this detailed study predicted the complexes with NCS and NCSe co-ligands also to have a low spin ground state. Since the effect of crystal packing including the role of the lattice solvent cannot be accounted for in the DFT calculations, we synthesised the solvatomorphs of the complexes with $L^{TetraPh-ODA}$ with all three NCE co-ligands where E=S, Se and BH_3 and investigated the effect of methanol as a lattice solvent in comparison to the previously reported acetonitrile analogues. To put the title in context: the term Hobson's choice is a common English expression used when there is only one option available. Since in Fe(II) complexes based on the 1,3,4-Oxadiazole ligand system, irrespective of the ligand substituents, co-ligands or the lattice solvent chosen, only the complexes with $NCBH_3$ show spin crossover the other two NCX (X=S and Se) lock the complexes in the HS state.

Experimental

All chemicals were purchased from Alfa Aesar, Deutero, Fisher Chemicals, TCI, Sigma-Aldrich, and Acros Organics and used without further purification. Solvents were dried according to the literature-known procedures and used freshly distilled.[19] Dry DMF was purchased from Sigma Aldrich. NMR spectra were recorded at room temperature with a Bruker Avance DSX 400 and analysed with the program MestReNova. Magnetic susceptibility measurements were performed on a Quantum Design SQUID magnetometer MPMSXL in a temperature range between 2 and 400 K with

[a] S. Sundaresan, J. Eppelsheimer, L. M. Carrella, E. Rentschler
Department Chemie, Johannes-Gutenberg-Universität Mainz, Duesbergweg 10–14, 55128 Mainz, Germany
E-mail: ssundare@uni-mainz.de
rentschler@uni-mainz.de

Supporting information for this article is available on the WWW under https://doi.org/10.1002/ejic.202400690

Research Article
doi.org/10.1002/ejic.202400690

an applied field of 1 kOe. All elemental analyses (Elementar vario EL Cube: C, H, and N) were measured at the microanalytical laboratories of the Johannes Gutenberg University Mainz. X-ray diffraction data were collected with a STOE STADIVARI at Johannes Gutenberg University Mainz. The structures were solved with ShelXT[20] and refined with ShelXL[21,22] implemented in the program Olex2.[23] The X-ray cif file data are deposited on the Cambridge CCDC database with identification numbers 2391192–2391194. The ligand $\mathbf{L^{Ph-ODA}}$ used for the complex synthesis was synthesized as previously recently reported by some of us in the literature.

Complex Synthesis

$[Fe^{II}(L^{Ph-ODA})(NCS)_2]\cdot 1.5H_2O\cdot 1.5CH_3OH$ (C1)

The following reaction was carried out in a glovebox under an inert atmosphere. $[Fe(py)_4(NCS)_2]$ (49 mg, 0.1 mmol, 1 eq) was dissolved in 3 ml methanol and stirred for 15 minutes. The solution was filtered with a syringe filter. The filtrate was added to a solution of $\mathbf{L^{Ph-ODA}}$ (36 mg, 0.1 mmol, 1 eq) in 2 ml methanol. The solution was kept undisturbed and set for slow evaporation of the solvent. After one week, yellow block-shaped crystals that were suitable for X-ray structure analysis had formed. The crystals were collected by filtration, washed with diethyl ether and dried at ambient pressure to afford $[Fe^{II}(\mathbf{L^{Ph-ODA}})(NCS)_2]$ (29.79 mg, 0.056 mmol, 56%) in moderate yields. FT-IR: $\tilde{\nu}$ (cm^{-1}) = 2907, 2849, 2058, 1970, 1602, 1572, 1554, 1479, 1439, 1387, 1351, 1314, 1300, 1284, 1245, 1153, 1121, 1098, 1069, 1042, 1018, 992, 975, 955, 927, 898, 881, 853, 817, 801, 779, 757, 735, 708, 689, 640, 510, 476, 419. Elemental Analysis calculated for $C_{23}H_{19}FeN_7O_1S_2\cdot 1.5H_2O\cdot 1.5CH_3OH$: C, 48.68; H, 4.67; N, 16.22. Found: C, 48.30; H, 4.42; N, 16.49.

$[Fe^{II}(L^{Ph-ODA})(NCSe)_2]\cdot 2.2H_2O\cdot 0.8CH_3OH$ (C2)

The following reaction was carried out in a glovebox under an inert atmosphere. $[Fe(py)_4(NCSe)_2]$ (58 mg, 0.1 mmol, 1 eq) was dissolved in 3 ml methanol and stirred for 15 minutes. The solution was filtered with a syringe filter. The filtrate was added to a solution of $\mathbf{L^{Ph-ODA}}$ (36 mg, 0.1 mmol, 1 eq) in 2 ml methanol. The solution was kept undisturbed and set for slow evaporation of the solvent. After five days, yellow block-shaped crystals suitable for X-ray structure analysis formed. The crystals were collected by filtration, washed with diethyl ether, and dried at ambient pressure to afford $[Fe^{II}(\mathbf{L^{Ph-ODA}})(NCSe)_2]$ **C2** in high yields(51.26 mg, 0.073 mmol, 82%). FT-IR: $\tilde{\nu}$ (cm^{-1}) = 3059 3026 2905 2854 2696 2065 1604 1571 1554 1482 1442 1384 1351 1312 1285 1248 1178 1154 1119 1098 1069 1051 1019 991 974 957 898 881 850 817 759 735 709 690 642 509 478 419. Elemental Analysis calculated for $C_{23}H_{19}FeN_7O_1Se_2\cdot 2.2H_2O\cdot 0.8CH_3OH$: C, 41.52; H, 3.89; N, 14.24. Found: C, 41.12; H, 3.79; N, 14.03.

$[Fe^{II}(L^{Ph-ODA})(NCBH_3)_2]\cdot 0.8H_2O\cdot 0.5CH_3OH$ (C3)

The following reaction was carried out in a glovebox under an inert atmosphere. $[Fe(py)_4(NCBH_3)_2]$ (45 mg, 0.1 mmol, 1 eq) was dissolved in 3 ml methanol and stirred for 15 minutes. The solution was filtered with a syringe filter. The filtrate was added to a solution of $\mathbf{L^{Ph-ODA}}$ (36 mg, 0.1 mmol, 1 eq) in 2 ml methanol. The solution was kept undisturbed and set for slow evaporation of the solvent. After one week, orange plate-shaped crystals suitable for X-ray structure analysis formed. The crystals were collected by filtration, washed with diethyl ether and dried at ambient pressure to afford $[Fe^{II}(\mathbf{L^{Ph-ODA}})(NCBH_3)_2]$ (**C3**) in moderate yields (29.33 mg, 0.053 mmol, 53%). FT-IR: $\tilde{\nu}$ (cm^{-1}) = 2980, 2928, 2338, 2179, 1605, 1575, 1558, 1541, 1521, 1507, 1488, 1477, 1457, 1445, 1425, 1419, 1305, 1244, 1154, 1124, 1113, 1096, 1054, 1045, 1020, 959, 940, 881, 852, 762, 738, 706, 688, 669, 644, 511, 493, 476, 417. Elemental Analysis calculated for $C_{23}H_{25}B_2FeN_7O_1\cdot 0.8H_2O\cdot 0.5CH_3OH$: C, 53.93; H, 5.51; N, 18.73. Found: C, 53.66; H, 5.31; N, 19.08.

Results and Discussion

The ligand 2-phenyl-5-[N,N bis(2-pyridylmethyl)aminomethyl]-1,3,4-oxadiazole ($\mathbf{L^{Ph-ODA}}$) was synthesised as reported earlier in high yields in five steps.[18] The ligand obtained was fully characterised using ^{1}H-NMR, ^{13}C-NMR, and infrared spectroscopy. The ligand obtained was to prepare three complexes **C1–C3** in methanol. All three complexes obtained were characterised using single crystal X-ray Crystallography, IR spectroscopy (Figures S21–S23), SQUID magnetometry and elemental analysis. The structural data were obtained from single crystals carefully picked from the mother liquor, whereas the bulk analysis, including elemental analysis and SQUID data were obtained from samples filtered and air dried from the mother liquor. During this process, some methanol present in the crystal lattice was replaced by water from the atmosphere, as often seen in the literature.[18]

Magnetic Data Analysis

The magnetic susceptibilities data for complex **C1** and **C2** were recorded on microcrystalline samples. The $\chi_M T$ data was recorded from 300–2 K in the cooling mode in both cases (Figure 1). The complexes in both cases stay in HS state with a $\chi_M T$ value of around 3.5 $cm^3\,mol^{-1}\,K$ which is in agreement with the literature values for mononuclear Fe(II) ranging from 3.0–4.0 $cm^3\,mol^{-1}\,K$. These findings are also in agreement with the average bond length of 2.18 Å for both complex **C1** and **C2** from the X-ray crystallography data obtained at 173 K, indicating that the complexes stay in the HS state. The sudden drop below 40 K in the $\chi_M T$ value can be explained by a combination of weak intermolecular dipolar interaction and weak zero-field splitting of the Fe(II) centre in both the cases. The magnetic

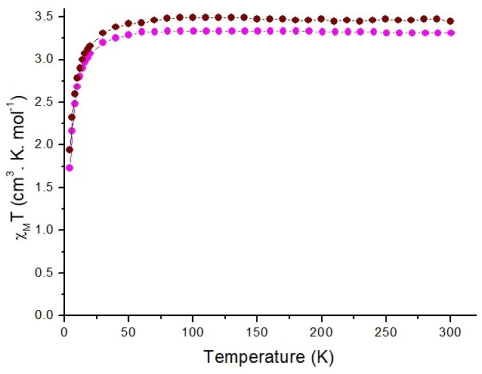

Figure 1. χ_MT *vs* T for complexes **C1**–**C2**. The dots are the data points, and the line is just a guide for the eye.

Research Article
doi.org/10.1002/ejic.202400690

behaviour of **C1** and **C2** complexes, locked in the HS state, is analogues to that of the previously reported acetonitrile solvatomorphs. This indicates that, irrespective of the lattice solvent chosen, the complexes with NCS and NCSe monodentate co-ligands stayed in HS state with the $\mathbf{L^{Ph-ODA}}$ ligand.[18] As previously stated, the reason for this solvatomorph investigation is to further probe the DFT results reported earlier on these systems. In the calculations a LS ground state was predicted for the complex with NCSe co-ligands.

Temperature dependent magnetic behaviour of **C3** was analysed in three sequential measurements. The sample was measured in the following sequences: (i) 300–90 K, (ii) 90–400 K and (iii) 400–2 K. The resulting $\chi_M T$ versus T plot is illustrated in Figure 2. At 300 K the $\chi_M T$ value is equal to 3.26 $cm^3 mol^{-1} K$ with a plateau down to 210 K. There is an abrupt transition centred around $T_{1/2}$ 166 K to LS state with a sudden drop in the $\chi_M T$ to 0.07 to $cm^3 mol^{-1}$ K at 130 K. Further heating to 300 K only leads to a slightly increased $\chi_M T$ product of 3.27 $cm^3 mol^{-1} K$.

At 400 K, the value of the HS species is 3.27 $cm^3 mol^{-1} K$. When cooling, the value begins to decrease already at 260 K and forms a plateau between 200 and 150 K. Below 150 K, the magnetic moment drops again significantly to a value of 0.28 $cm^3 mol^{-1} K$ at 130 K. Further cooling to 10 K results in the constant $\chi_M T$ value of approximately 0.16 $cm^3 mol^{-1} K$. At very low temperatures, the magnetic moment finally drops to 0.07 $cm^3 mol^{-1} K$ at 2 K. This temperature dependent behaviour of $\chi_M T$ illustrates a two-step spin crossover from the HS to the LS state via an intermediate state. Considering the $\chi_M T$ product of 0.2 $cm^3 mol^{-1} K$ at low temperatures, 95% of the HS molecules transitioned to the LS state. The final drop of the magnetic moment below 10 K might be ascribed to ZFS of the remaining $S=2$ high-spin molecules. The transition temperatures of the two-step SCO ($T_c^{\downarrow(2)} = 215$ K and $T_c^{\downarrow(3)} = 137$ K) are nearly equally distributed around the original transition temperature of $T_c^{\downarrow(1)} = 166$ K. The two–step SCO is most likely a result of the heating process towards 400 K and loss of the lattice solvent molecule. In the case of the acetonitrile solvatomorph reported earlier, complex was stuck in HS state upon solvent removal. The effect of solvatomorphism is well studied and investigated in the literature.[7,9] In addition, solvatomorphs of a SCO active compound might behave differently after annealing at 400 K. The crystals of **C3** were not suitable for singe-crystal X-ray structure analysis after being heated to high temperatures. Thus, a comparison of crystal structures was not possible. In order to still make a qualitative statement about the crystalline phases before and after the loss of solvents, powder X-ray diffraction (PXRD) was attempted to be employed. However, this was only successful for a freshly prepared sample of **C3** before temperature treatment. Upon solvent loss, the sample lost its crystallinity and PXRD measurement was not successful.

Structural Determination

All three complexes **C1–C3** are crystallised from methanol as yellow block solid by slow evaporation. The complexes are isostructural to their previously reported acetonitrile solvatomorphs. The X-ray data collected for complexes **C1** and **C2** at 173 K reveal that the complexes stay in HS state with an average bond length of 2.18 Å.[24–27] The excess electron density attributed to one methanol solvent was not possible to be resolved because of the disorder so a routine SQUEEZE was applied to remove them in the case of **C1**. Careful examination of the crystal packing clearly indicates the methanol solvatomorphs have crystal packing different from the acetonitrile analogues reported earlier. In the case of the complex **C3** (Figure 3), due to the disorder in the solvent molecule, a routine SQUEEZE was applied to remove electron density accounting for 32 electrons per asymmetric unit which accounts for approximately two methanol. The average metal to ligand bond distance at 173 K of 1.98 Å indicates the complex stays in LS state. Variable temperature X-ray structure analysis was not possible. Metal donor bond distances for all three complexes are tabulated in Table 1. All the other important X-ray crystallography parameters are tabulated in Tables S1–S4.

Three unique intermolecular π-π interactions can be found. The first parallel π-π stacking takes place between two pyridine rings of two adjacent molecules, which results in a one-dimensional chain along the b-axis (Figure S16) similar to the analogue acetonitrile solvatomroph.[18] Since the oxadiazole-

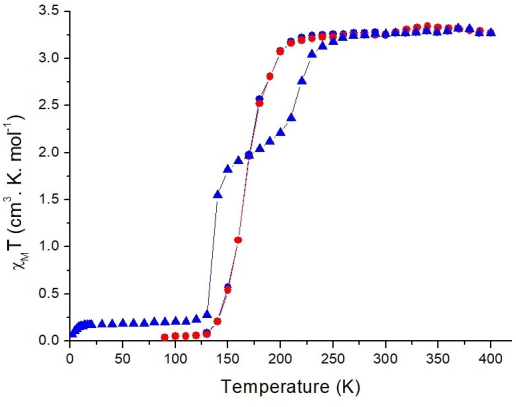

Figure 2. $\chi_M T$ *vs* T for complexes **C3**. 300–90 K blue dots, 90–400 K red dots, 400–2 K blue triangles. The lines are only a guide for the eye.

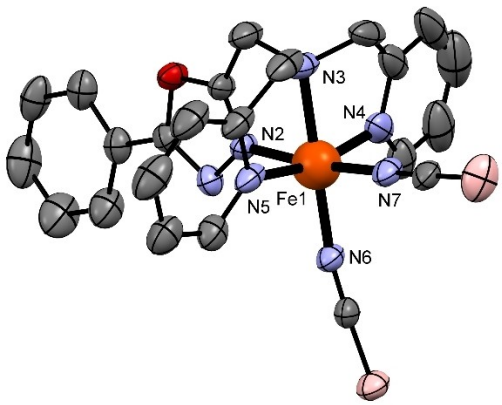

Figure 3. Crystal structure of $[Fe^{II}(\mathbf{L^{Ph-ODA}})(NCBH_3)_2]\cdot 0.8H_2O\cdot 0.5CH_3OH$ (**C3**).

Research Article
doi.org/10.1002/ejic.202400690

Table 1. Metal donor bond length of complexes **C1–C3** at 173 K.

Bond/Å	C1	C2	C3
	173 K	173 K	173 K
Fe–N1	2.2082(12)	2.198(2)	1.979(5)
Fe–N2	2.3028(11)	2.2897(19)	2.045(5)
Fe–N3	2.2149(12)	2.196(2)	1.985(6)
Fe–N4	2.1996(12)	2.208(2)	1.970(6)
Fe–N5	2.1143(13)	2.118(2)	1.952(5)
Fe–N6	2.0487(12)	2.063(2)	1.936(5)
$\overline{Fe-N}$	2.18	2.18	1.98

phenyl residues are approximately orthogonal to the chain direction, they can stack with the oxadiazole-phenyl fragments of neighbouring chains. In addition to that, a T-shaped π-π interaction between the phenyl ring and a pyridine moiety can be found between two chains. This type of crosslinking results in an intermolecular connection of the complex molecules in two dimensions. Thus, in, a two-dimensional network of complex molecules *via* π-π interactions is formed in the crystalline phase. All relevant π-π interactions parameters are tabulated in Table S5. As in the case of the **C3** complex, the packing diagrams shown in Figure 4 reveal chains of complexes along the *b*- and *c*-axis, with spaces in between where the solvent molecules squeezed during the structure refinement are located. This change in packing compared to the acetonitrile solvate form could be responsible for change in the magnetic behaviour.

Conclusions

In this work, we have successfully synthesised three methanol solvatomorph complexes (**C1–C3**) of previously reported acetonitrile analogues and investigated how variations in crystal packing affect the spin-crossover behaviour. Complexes **C1** and **C2**, with NCS and NCSe co-ligands, remain in the high-spin (HS) state over the entire measured temperature range, while complex **C3**, with the $NCBH_3$ co-ligand, exhibits an abrupt spin transition with a $T_{1/2}$ of 166 K. Upon heating the $NCBH_3$ complex to 400 K and removing the lattice solvent, the spin-transition property was retained and exhibited a stepped spin transition with $T_{1/2}(1)$ at 215 K and $T_{1/2}(2)$ at 137 K. Our results confirm that the ligand field strength of the NCS and NCSe co-ligands is significantly weaker compared to that of $NCBH_3$. Only the latter co-ligand along with $\mathbf{L}^{\mathbf{Ph-ODA}}$ yields the appropriate ligand field for the SCO in this system. On the other hand, it is important to note that subtle changes caused by the crystal lattice of the complex with $NCBH_3$ coligand (variation in the lattice solvent and packing) cause the difference in the SCO behaviour exhibited. This is why, this class of molecular materials are promising candidates for applications such as solvent sensors.

Acknowledgements

All the authors sincerely thank JGU Mainz for the funding and support. Open Access funding enabled and organized by Projekt DEAL.

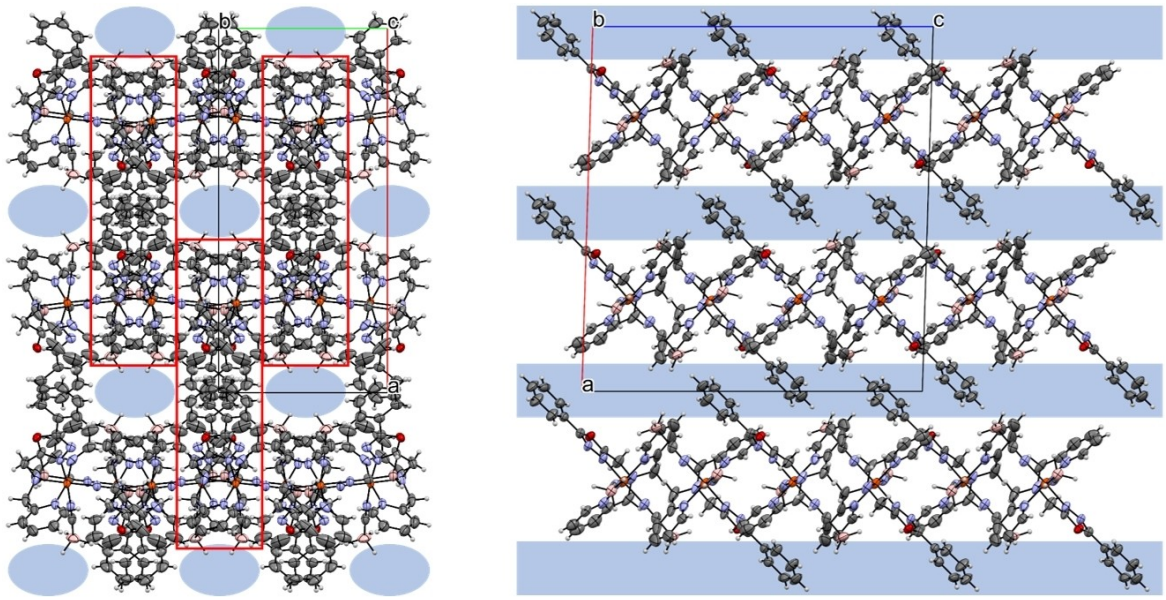

Figure 4. Packing of **C3** with view along the c-axis (left) and view along the b-axis (right). Red rectangles mark the one-dimensional chains of complex molecules along the c-axis. Blue areas illustrate the channel of solvent molecules. Colour scheme: pink – B, dark grey – C, grey – H, violet – N, red – O, orange – Fe. ORTEP representation with atomic displacement parameters set to 50% probability.

Research Article
doi.org/10.1002/ejic.202400690

Conflict of Interests

There are no conflicts of interest to declare.

Data Availability Statement

The data that support the findings of this study are available from the corresponding author upon reasonable request.

Keywords: SCO · Solvatomorphism · Iron · 1,3,4-Oxadiazole

[1] M. A. Halcrow, *Spin-Crossover Materials: Properties and Applications*, John Wiley and Sons, **2013**.
[2] A. B. Gaspar, M. Seredyuk, *Coord. Chem. Rev.* **2014**, *268*, 41–58.
[3] K. Senthil Kumar, M. Ruben, *Angew. Chem. Int. Ed.* **2021**, *60*, 7502–7521.
[4] N. A. A. M. Amin, S. M. Said, M. F. M. Salleh, A. M. Afifi, N. M. J. N. Ibrahim, M. M. I. M. Hasnan, M. Tahir, N. Z. I. Hashim, *Inorg. Chim. Acta* **2023**, *544*, 121168.
[5] K. S. Woo, A. Zhang, A. Arabelo, T. D. Brown, M. Park, A. A. Talin, E. J. Fuller, R. Singh Bisht, X. Qian, R. Arroyave, S. Ramanathan, L. Thomas, R. S. Williams, S. Kumar, *Nat. Commun.* **2024**, *15*, 4656.
[6] A. Tsukiashi, K. Sik Min, H. Kitayama, H. Terasawa, S. Yoshinaga, M. Takeda, L. F. Lindoy, S. Hayami, *Sci.Rep.* **2018**, *8*, 14911.
[7] M. Steinert, B. Schneider, S. Dechert, S. Demeshko, F. Meyer, *Inorg. Chem.* **2016**, *55*, 2363–2373.
[8] C. F. Herold, S. I. Shylin, E. Rentschler, *Inorg. Chem.* **2016**, *55*, 6414–6419.
[9] U. Habarakada, T. Boonprab, P. Harding, K. S. Murray, W. Phonsri, S. M. Neville, M. Ahmed, D. J. Harding, *Cryst. Growth Des.* **2022**, *22*, 4895–4905.
[10] C. M. Jureschi, J. Linares, A. Boulmaali, P. R. Dahoo, A. Rotaru, Y. Garcia, *Sensors* **2016**, *16*, 187.
[11] D. Gentili, N. Demitri, B. Schä, F. Liscio, I. Bergenti, G. Ruani, M. Ruben, M. Cavallini, *J. Mater. Chem. C* **2015**, *7836*, 7844.
[12] K. Senthil Kumar, M. Ruben, *Coord. Chem. Rev.* **2017**, *346*, 176–205.
[13] C. Köhler, E. Rentschler, *Eur. J. Inorg. Chem.* **2016**, 1955–1960.
[14] S. Sundaresan, J. Eppelsheimer, L. M. Carrella, E. Rentschler, *Crystals* **2022**, *12*, 404.
[15] P. Zoufalý, A. Kliuikov, E. Čižmár, I. Císařová, R. Herchel, *Eur. J. Inorg. Chem.* **2021**, 1190–1199.
[16] J. Klingele, D. Kaase, M. Schmucker, Y. Lan, G. Chastanet, J. Letard, *Inorg. Chem.* **2013**, *52*, 6010.
[17] S. Sundaresan, J.-G. Becker, J. Eppelsheimer, A. E. Sedykh, L. M. Carrella, K. Müller-Buschbaum, E. Rentschler, *Dalton Trans.* **2023**, *52*, 13181–13189.
[18] S. Sundaresan, J. Eppelsheimer, E. Gera, L. Wiener, L. M. Carrella, K. R. Vignesh, E. Rentschler, *Dalton Trans.* **2024**, *53*, 10303–10317.
[19] W. L. F. Armarego, *Purification of Laboratory Chemicals*, **2017** 7th ed.; Elsevier: Oxford, 2017; pp. 95–634.
[20] G. M. Sheldrick, *Acta Cryst.* **2015**, *71*, 3–8.
[21] G. M. Sheldrick, T. R. Schneider, *Methods Enzymol.* **1997**, *277*, 319–343.
[22] G. M. Sheldrick, *Acta Crystallogr. A* **2008**, *64*, 112–122.
[23] O. V Dolomanov, L. J. Bourhis, R. J. Gildea, J. A. K. Howard, H. Puschmann, *J. Appl. Cryst.* **2009**, *42*, 339–341.
[24] C. Lochenie, K. Schötz, F. Panzer, H. Kurz, B. Maier, F. Puchtler, S. Agarwal, A. Köhler, B. Weber, *J. Am. Chem. Soc.* **2018**, *140*, 700–709.
[25] P. Gütlich, Y. Garcia, H. A. Goodwin, *Chem. Soc. Rev.* **2000**, *29*, 419–427.
[26] H. S. Scott, R. W. Staniland, P. E. Kruger, *Coord. Chem. Rev.* **2018**, *362*, 24–43.
[27] S. Rodríguez-Jiménezjiménez, S. Brooker, *Inorg. Chem.* **2017**, *56*, 13697–13708.

Manuscript received: October 17, 2024
Revised manuscript received: December 20, 2024
Accepted manuscript online: February 4, 2025
Version of record online: February 25, 2025